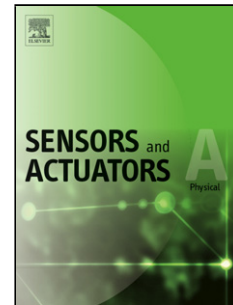


Accepted Manuscript

Title: Nanostructured functional Ti-Ag electrodes for large deformation sensor applications

Author: A. Ferreira C. Lopes N. Martin S. Lanceros-Méndez
F. Vaz



PII: S0924-4247(14)00436-1
DOI: <http://dx.doi.org/doi:10.1016/j.sna.2014.09.031>
Reference: SNA 8919

To appear in: *Sensors and Actuators A*

Received date: 30-5-2014
Revised date: 12-8-2014
Accepted date: 30-9-2014

Please cite this article as: A. Ferreira, C. Lopes, N. Martin, S. Lanceros-Méndez, F. Vaz, Nanostructured functional Ti-Ag electrodes for large deformation sensor applications, *Sensors and Actuators: A Physical* (2014), <http://dx.doi.org/10.1016/j.sna.2014.09.031>

This is a PDF file of an unedited manuscript that has been accepted for publication. As a service to our customers we are providing this early version of the manuscript. The manuscript will undergo copyediting, typesetting, and review of the resulting proof before it is published in its final form. Please note that during the production process errors may be discovered which could affect the content, and all legal disclaimers that apply to the journal pertain.

Nanostructured functional Ti-Ag electrodes for large deformation sensor applications

A. Ferreira¹, C. Lopes¹, N. Martin², S. Lanceros-Méndez¹, F. Vaz^{1*}

1- Centro/Dept. de Física da Universidade do Minho, 4710-058 Braga, Portugal.

2 - Institut FEMTO-ST, UMR CNRS 6174 – Université de Franche Comté – CNRS – ENSMM – UTBM, 32, Avenue de l'observatoire, 25044 Besançon Cedex, France.

*Corresponding author: fvaz@fisica.uminho.pt; fax: (+351)253604398; phone: (+351)253510471

Abstract

This paper reports on the development of thin film-based stretchable electrodes, suitable for different types of sensors. Columnar Ti-Ag thin films with a Ag content of 8 at.% were prepared by D.C. magnetron sputtering on carbon nanotube/poly(vinylidene fluoride) CNT/PVDF piezoresistive composites. *GLancing Angle Deposition*, GLAD, technique was used to change the typical normal columnar growth microstructure obtained by conventional sputtering, into different growing architectures, such as inclined columns and zigzag profiles, in order to tune mechanical and electrical responses of the materials. Three different incident angles of the particle flux, $\alpha = 40^\circ$, 60° and 80° , were used to deposit Ti-Ag thin films with the different architectures. Upon uniaxial stretching of the prepared zigzag thin films, the resistance of the thin film starts increasing smoothly for strains up to 3%. Above 10% strain, a sharp increase of the electrical resistance is observed due to film mechanical failure and therefore interruption of the electrical conductivity pathways. Furthermore, the influence of the thin film architecture was also studied with respect to the performance of piezoresistive sensors based on carbon nanotube/poly(vinylidene fluoride), CNT/PVDF, composites in which Ti-Ag coated films served as electrodes for signal acquisition. Electromechanical tests were thus performed in composites with CNT contents close to the percolation threshold, where the electromechanical response, characterized by the Gauge Factor, is the largest. The stability of the piezoresistive response was analyzed for the various architectures of the GLAD sputtered Ti-Ag electrodes, including incident angle and number of zigzag periods. It is shown that thin film architecture has a pronounced influence in the overall sensor response,

where the best results are obtained for piezoresistive polymer composites coated with Ti-Ag films, produced with intermediate ($\alpha = 60^\circ$) incident angles.

Keywords: Stretchable electrodes, piezoresistive sensors, GLAD, Ti-Ag thin films, polymer composites, PVDF, CNT.

1. Introduction

In the fields of sensing and actuating devices [1, 2] the use of polymer based materials allows to develop smart materials and functional composites by the production of conductive polymer composites, using small amounts of carbon nanotubes – CNT – dispersed in an insulating polymer matrix. In particular, composite materials can be developed with the ability to change significantly the electrical response when subjected to strains, which is suitable for the development of high sensitive polymer-based strain sensors [1-3]. However, one of the critical issues of these sensors is the reliability of the electrodes, which link the responsive polymer composite to the signal acquisition circuit. This is particularly challenging given the relatively high and complex mechanical solicitation expected for these applications, i.e. bending, elongation and torsion. In fact, these sensors must be reliable and retain reproducibility and structural integrity over their lifetime. Furthermore, corrosive and mechanical failures must not occur. Thus, these materials, though not selected exclusively at the base of their mechanical and chemical properties, must provide adequate mechanical and chemical resistance that arise in any given application. Several technologies have been proposed to develop suitable electrodes for large strain sensors, including the use of intrinsic conductive polymers [4, 5], pre-stressed metal conductors [6, 7] or in plane patterned metal conductors [8, 9]. Metals can be deposited in thin layers on a broad range of substrates by electron beam evaporation, cathodic sputtering or electroplating and patterned down to the nm scale using photolithographic processes [10]. These processes are the best options to realize these electrodes due to their large electrical conductivity and relatively low cost, the main challenge remaining to maintain the integrity of the signal acquisition electrodes for larger deformations and repeated loading cycles. Further, reproducible results at a large production throughput must be obtained with the potential of moving the technology from the lab to the industry. The ability to pattern the electrodes on a small scale allows the fabrication of many electrically independent sensors and/or actuators on the same coating process, which paves the way for a broad range of novel applications.

In order to produce such electrodes, there are two major obstacles to the direct use of metallic

thin film:

1. the Young modulus of metals is some orders of magnitude higher than that of polymers (50–100 GPa compared to 0.2–1 MPa) [11];
2. the limit of elasticity for metals is around 2% and if a metal electrode is strained above this limit it will crack and strongly reduce the electrical conductivity [11].

Beyond the specific nature and characteristics of the chosen smart polymer based sensing material, the approach reported in this work consists in using a sputtered conductive thin layer to detect the strain-induced electric signal produced by the reversible mechanical deformation in the polymer composite. The selected layer system should reveal high corrosion and wear resistance, high conductivity and high elasticity (deformation resistance) and, additionally, good chemical, thermal and mechanical stability. Therefore, the metallic film to coat the polymeric sensor, as well as the production method, should be carefully selected. Based on previous works [12, 13] and given the large potential of these materials in the biomedical field, the Ti-Ag system was chosen to coat the polymers. Ti-Ag thin films combine the excellent Ti biocompatibility with the Ag antimicrobial properties, offering good thermal, electrical, chemical and mechanical properties, together with good wear and corrosion resistance [14-16].

Concerning the thin film preparation, it is known that the microstructure of the films strongly depends on the experimental parameters used during film deposition [17-20]. In conventional Physical Vapor Deposition (PVD) techniques, the normal incidence of the particle flux leads to a typically columnar growth normal to the substrate. Offering strong benefits comparatively to the conventional sputtering techniques, the Glancing Angle Deposition technique (GLAD), first reported in 1959 [21], is a suitable way to modify the microstructural aspects of the thin film and, indirectly the physico-chemical properties. Indeed a wide range of morphologies can be tailored by combining oblique incidence of the depositing species and substrate motion.

This work reports on how the evolution of the morphological features of the GLAD sputtered Ti-Ag thin films can affect its electrical, mechanical and electromechanical responses, as they will influence sensor response and reliability.

2. Experimental details

2.1. Processing of the materials

2.1.1. Carbon nanotube/poly(vinylidene fluoride) piezoresistive composites

The CNT/PVDF piezoresistive composites were prepared following the procedure described in [22]. In short, the appropriate amount of CNT, (Single Walled CNT, SWCNT, AP-SWNT grade) were purchased from Carbon Solutions Inc., Riverside, California, was mixed with 15 to 20 mL of acetone and immersed in an ultrasound bath. Separately, PVDF was manually dispersed in acetone and then added to the SWCNT/acetone dispersion, in an ultrasound bath [23]. The total mass of PVDF and CNT sample was approximately 11 g. A mechanical stirrer was inserted into the acetone dispersion and sonication and mechanical stirring were applied until the acetone was completely evaporated. The resulting material was cut into small pellets and pressed at 2 Tons and 200 °C for 1 h. The material was let to cool down inside a mould. The nonpolar α -phase was obtained by crystallization from the melt. Homogeneous discs, with diameters of 130 mm, thicknesses of 1 mm and CNT filler contents between 0 (blank samples - just PVDF - to serve as a reference in the thin film conductivity measurements) and 10 wt.% were obtained.

2.1.2. Ti-Ag thin films

Ti-Ag thin films were deposited by D.C. reactive magnetron sputtering inside a stainless-steel custom-made vacuum reactor with a volume of 40 L. The reactor, equipped with a circular planar and water cooled magnetron sputtering source, was evacuated with a turbomolecular pump, backed by a mechanical pump, in order to obtain an ultimate pressure of 10^{-5} Pa. A titanium target (purity 99.6 at.%, 51 mm diameter) was used and 11 inserts of silver (purity 99.9 at.%, 2 mm diameter) were placed equidistant from each other, within the preferential erosion zone of the target. This amount of pellets was used to obtain a Ag amount between 5 and 10 at.%, which was found to be in a good composition range for the present large deformation sensor applications [12, 13]. The composite target was sputtered under a pure argon atmosphere, with a constant flow rate of 2.4 sccm, corresponding to a total pressure of 0.3 Pa. The pumping speed was set constant at $S = 10 \text{ L s}^{-1}$. Before each deposition, the CNT/PVDF samples were cleaned with ethanol and introduced through a 1 L airlock. In order to remove the target surface contamination layer, a pre-sputtering of the composite target was performed for 5 min. Finally the samples were positioned at 50 mm from the target and grounded. The depositions were carried out at room temperature and the Ti-Ag composite target powered with a constant current density of 24.5 A.m^{-2} . The deposition time

was adjusted in order to obtain a thickness range between 400 nm and 900 nm. There is a linear dependence between film thickness and deposition time, which was previously studied by the determination of the deposition rate for each one of the individual film architecture, described below. All the sputtering parameters were optimized taking into account the strong changes in the mechanical behaviour of the polymer that occurs at $\sim 90^{\circ}\text{C}$ [24].

The composition of the prepared films was measured by Rutherford Backscattering Spectrometry (RBS). The measurements were carried out using a ^4He with 2 MeV and a ^1H with 2.3 MeV beams, at an angle of incidence 0° . Three detectors were used, one standard located at 140° , and two pin-diode detectors located symmetrical each other, both at 165° . Composition profiles for the as-deposited samples were determined using the software NDF [25, 26]. The error associated to the Ag concentration was about 0.5 at.%, according to the resolution of this technique.

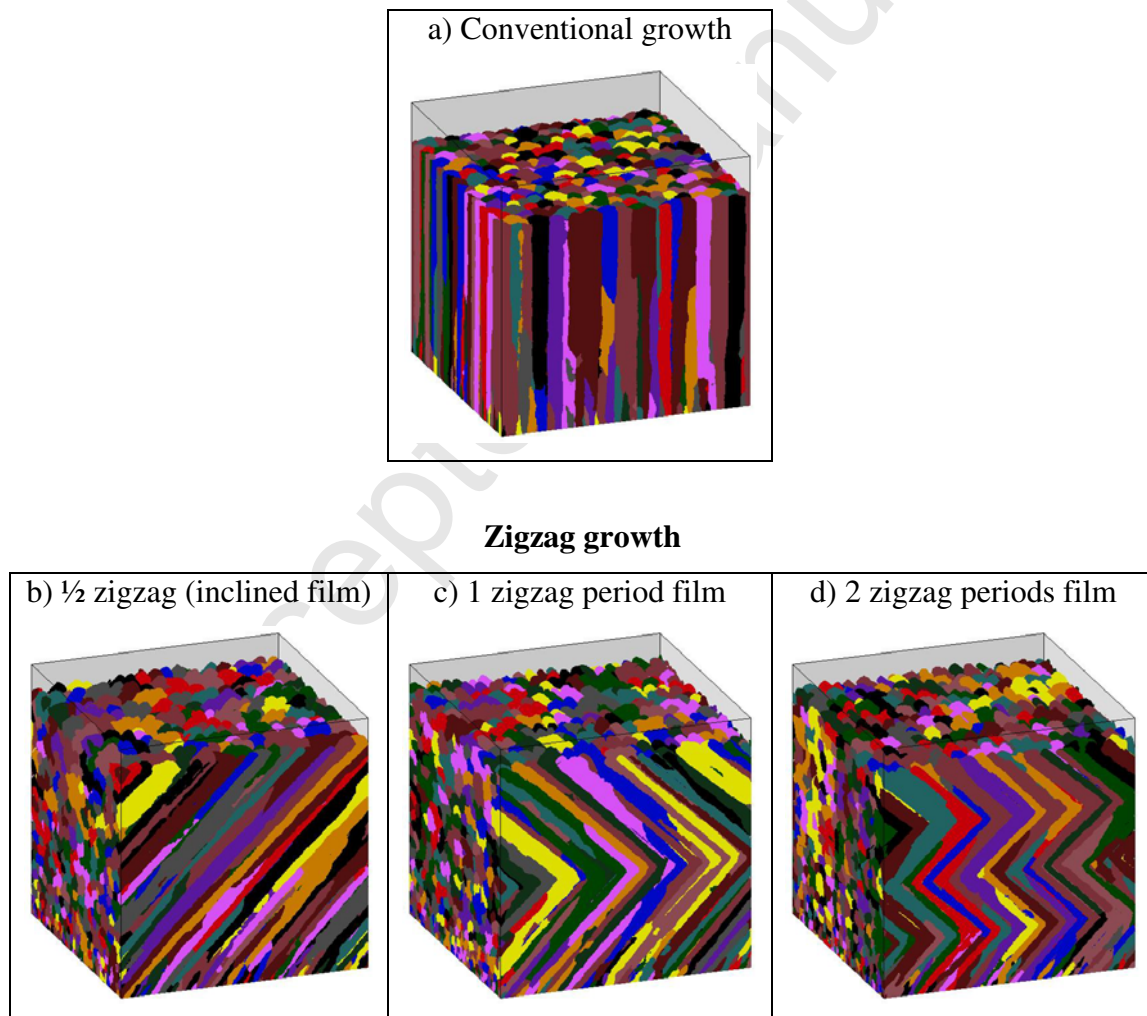


Figure 1 - Schematic representation of the thin film microstructural features.

In order to study the change in the electromechanical response of the thin films, a set of different architectures were tailored by varying the direction of the incident particles flux.

Four different types of films were grown in order to correlate the growth conditions (conventional and zigzag approaches) and the specific features of the GLAD-like prepared films with the response of the thin films and piezoresistive composites. Figure 1 shows a schematic illustration of the different prepared films and their main microstructural features. PVD techniques use normal incidence to obtain the typical columnar growth normal to the deposition substrate, Fig. 1a). With adequate operating conditions, GLAD technique allows obtaining columnar microstructures with specific architectures by controlling the orientation of the substrate relative to the impinging vapor flux, as illustrated in Fig. 1b), 1c) and 1d). In the observed columns, when the incident angles of the particles flux α increase with respect to the sample surface, the angle β of the column with respect to the sample surface, increases the same way.

2.2. Electrical resistance measurements

Two different electrical conductivity measurements were performed in the samples. Electrical resistance of the CNT/PVDF composites was calculated from the slope of I–V curves, measured at room temperature with an automated Keithley 487 picoammeter/voltage source. I–V data points were collected between Au contacts, deposited on both sides of the samples with a Polaron SC502 sputter coater. Volume resistivity was measured with circular contacts of 5 mm diameter with an applied voltage ranging between ± 10 V and measuring the current. The resistivity ρ (Ωm) was calculated by [27]:

$$\rho = \frac{R \cdot A}{d} \quad (1)$$

where R is the resistance of the composite (Ω), d the thickness (m) and A the area of the electrodes (m^2).

Second, the electrical conductivity of Ti-Ag thin films was measured at room temperature, using the four-probe van der Pauw method [28, 29]. The measurements were carried out in a custom-made dark chamber. The error associated to the electrical measurements is below 1%.

2.3. Electromechanical characterization

Electromechanical tests were performed considering the whole system: CNT/PVDF polymer coated with the Ti-Ag thin films. The electrical resistance of the samples (approximate

dimensions: $60 \times 10 \text{ mm}^2$ and $\sim 1 \text{ mm}$ of thickness) was measured through the Ti-Ag electrodes with an Agilent 34401A multimeter during the mechanical deformation of the sample, applied with an universal testing machine from Shimadzu (model AG-IS, with a load cell of 1 kN).

Two different mechanical solicitations were applied to the samples. During the so-called method 1, mechanical experiments were performed in the tensile mode (Fig. 2a); in the method 2, 4-point-bending deformation was applied to the samples (Fig. 2b).

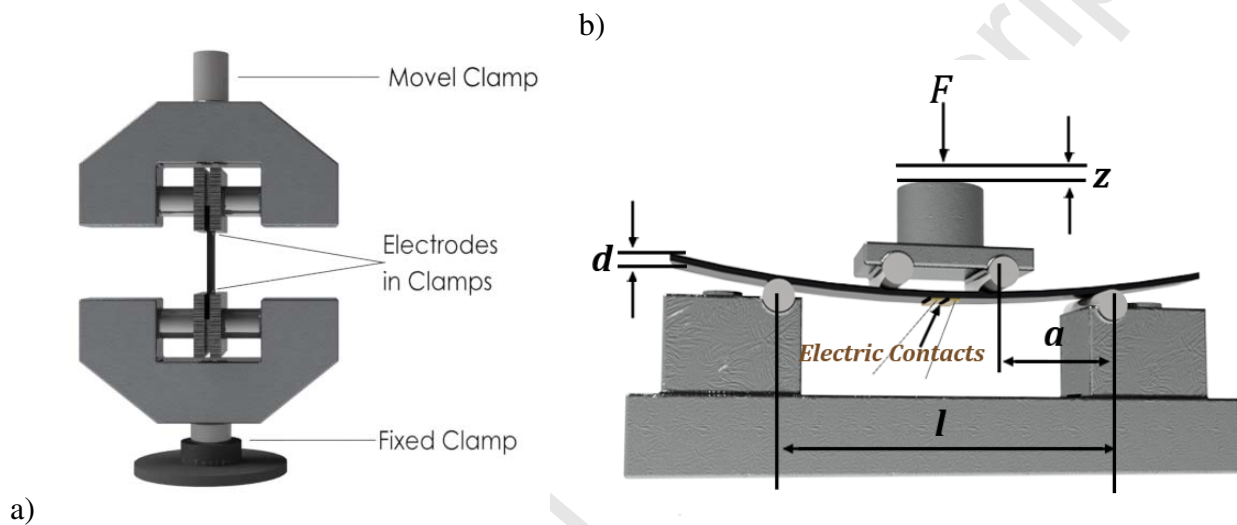


Figure 2 - Schematic representation of the experimental configuration of the a) clamps for the stress-strain uniaxial stress experiments (method 1) with simultaneous electrical measurements for electrical response evaluation of the samples and b) representation of the 4-point bending tests (method 2) apparatus where z is the vertical displacement, d is the thickness of the sample and a is the distance between the first and the second bending points (15 mm). The electrodes are in the center of the sample.

The evaluation of the electrical resistance response during the uniaxial stress tests (Fig. 1) was performed at speed rate of 0.5 mm/min and at a maximum strain level of 10%.

For the 4-point-bending measurements (Fig. 2b), the Ti-Ag electrodes with an area of $10 \times 1 \text{ mm}^2$, were placed at the bottom of the sample. For all experiments, 4 loading-unloading cycles were performed and the average electromechanical response was evaluated. All these experiments were carried out at room temperature.

2.4. Morphological analysis

The morphological features of the Ti-Ag thin films was probed by scanning electron microscopy (SEM). Cross-section micrographs were obtained at room temperature in a FEI Quanta 400FEG ESEM apparatus operating at 15 keV.

Additional information about surface properties (roughness and surface morphology) was obtained by atomic force microscopy (AFM), using a MultiMode STM microscope controlled by the Nanoscope III (tapping mode) system. The measurements were performed over surface scan areas of $5 \times 5 \mu\text{m}^2$.

3. Results and discussion

3.1. Electrical properties of Ti-Ag electrodes

All prepared films were found to have a Ag content of about 8 at.%, measured by RBS. In order to study the electrical properties of the Ti-Ag electrodes sputtered by GLAD, electrical resistivity measurements at room temperature were carried out. The electrical behavior of the Ti-Ag thin films is presented in Fig. 3, where the influence of the different processing parameters -number of zigzag periods and sputter angles- was analyzed.

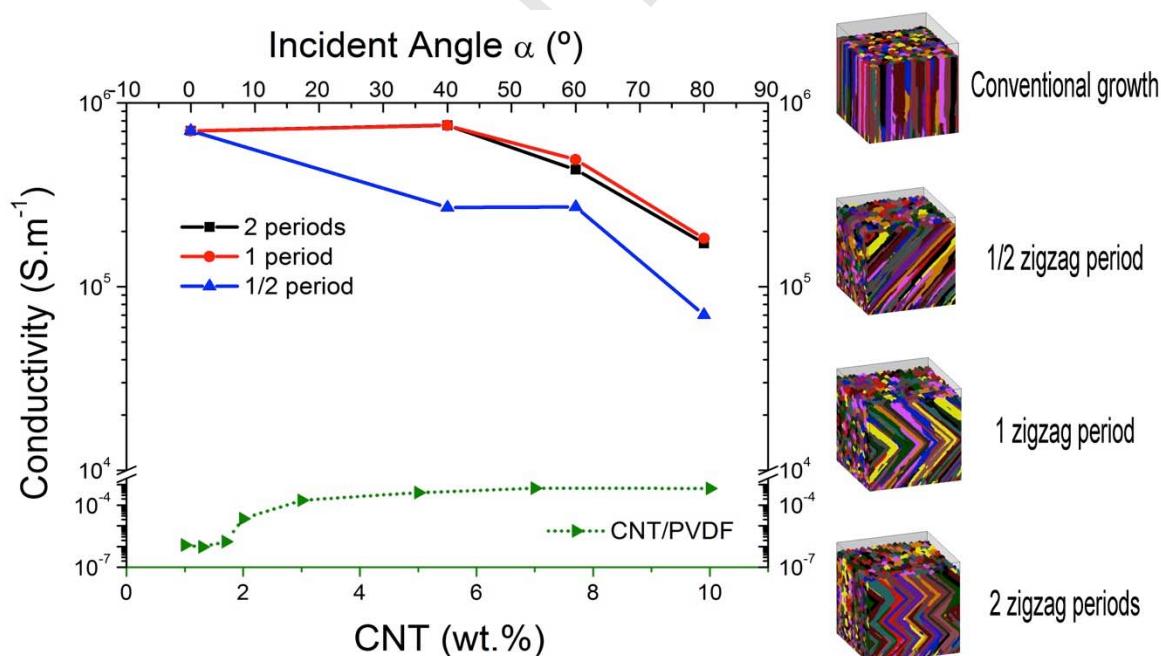


Figure 3 - Electrical conductivity of Ti-Ag films as a function of the incident angle (α) and the number of periods, and electrical conductivity of polymer composite as a function of CNT (wt.%).

The results plotted in Fig. 3 show that the films are characterized by suitable electrical conductivity for sensor electrode applications, with varying properties depending on the

number of periods and, mainly, deposition angle. The Ti-Ag thin films exhibit conductivity values in the order of 10^5 S.m^{-1} , smaller than the bulk Ti around 10^6 S.m^{-1} [30], and several orders of magnitude higher than the polymer composite (10^4 S.m^{-1}) and thus adequate to be used as electrodes. Further, a slight enhancement of the electrical conductivity is observed for the lowest incident angles ($\alpha = 40^\circ$) and for the highest number of periods (Fig. 3), which is correlated with changes in the grain boundaries, in particular with the voids between the columnar structures. These voids are promoted as the incident angle increases and therefore the column angle β increases [31, 32].

The effects of Ag additions to a stoichiometric TiN matrix has been studied [33] and it is reported that for intermediate Ag contents (between ~6 and ~20 at.%), highly conductive Ag particles are placed among the TiN columns, providing an increased number of conduction paths. Further, in the case of the inclined features, the increase of both α and β angles give rise to increased porosity [34]. Thus, scattering at the column's interface is favoured, which reduces the electronic transport properties of the coatings [34]. Additional parameters such as temperature (T), film thickness (d), grain size (D) and the mean free path of the electrons in the film (λ_e) also affect the electrical conductivity (σ) of the metallic thin films [31]. These parameters are also correlated with changes in the grain boundaries, mainly in the column frontiers, which behave as a potential barrier, which decreases the probability of the electron transmission [31]. Thus, the variations in the electrical conductivity are mainly due to the modifications on the film's architecture and growing conditions. As demonstrated in [35], the major contribution to the total resistivity comes from electron scattering at grain boundaries and therefore to the significant modifications of the film's morphology.

3.2. Electrical behaviour of Ti-Ag films under uniaxial stretching

To minimize the overall stiffness of the sensors, materials for both the matrix and the electrically active components should have low Young modulus and an ability to accommodate large strain deformations with a linear, elastic response. Thus, mechanical response and electrical transport properties are important.

Regarding the thin films prepared within the frame of this work, the electrical resistance for deformations up to 10% along the axial direction of the incident angle are shown in Fig. 4.

a)

b)

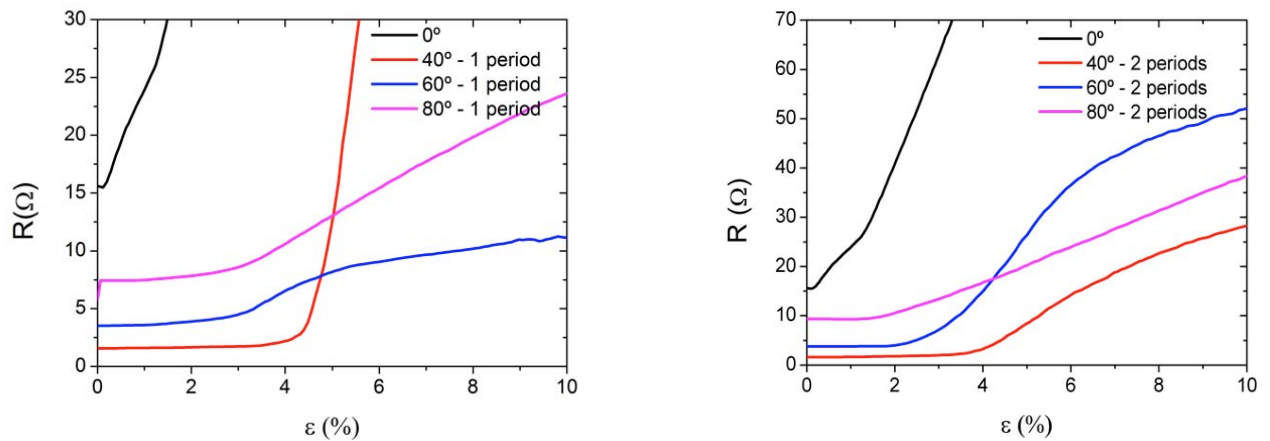


Figure 4 - Electrical resistance as a function of the tensile strain ε of the sputtered Ti-Ag samples for the different incident angles $\alpha = 0, 40, 60$ and 80° and geometries: a) 1 zigzag period; b) 2 zigzags periods.

The results plotted in Fig. 4 reveal two very distinct behaviors. On the one hand, the thin films deposited in the conventional way ($\alpha = 0^\circ$) show a very poor resistance to stretching, with the electrical resistance increases sharply after the application of the deformation. As shown in Fig. 4, upon uniaxial stretching, the samples deposited in conventional approach ($\alpha = 0^\circ$) reveal that the resistance starts increasing immediately after the stretching started, which demonstrates its inadequacy for the targeted sensor applications. This undesirable behaviour is actually expected as demonstrated in [9, 11], where electrodes produced with conventional sputtering deposition resulted in the smallest strain range before loss of conductivity, which was limited to $\varepsilon = 3\%$. At 1% strain, cracks started to appear perpendicularly to the stretch direction, and the cracks became wide enough to completely interrupt the conducting path for strains of 3%. On the other hand, to solve this limitation, patterning metal traces can be used [9, 10, 36]. When carefully designed, the patterned electrode still allows for the polymer to move and expand in the desired direction without damaging the metallic thin-film.

For the prepared zigzag structures, the resistance starts increasing only for strain ranging from 2 to 3% (Fig. 4). Furthermore, and even for the higher strain, the surface resistance increases smoothly, mainly due to a geometrical effect, demonstrating the large difference with respect to the conventional deposited films. A sharp increase of the electrical resistance occurs only above 10% strain, indicating electrical conductivity failure due to film damage (Fig. 4).

The structures with 2 periods (4 zigzags) presented in Fig. 4b) show no relevant variations of the electrical resistance for strains of $\sim 4\%$ for an incident angle of 40° . On the other hand,

the resistance of the samples prepared with $\alpha = 60^\circ$ show variations of the electrical resistance for stretching around 3%. However, it is worth to note that these samples also showed a better strain distribution, with just a small increase of resistance up to 10% strain, allowing their use for high strain sensor applications. Failure is expected in regions where the highest plastic strain concentration is located [9, 11]. In a general way, an increase of the incident angle and the number of zigzags promotes a reduction in the accumulated strain (Fig. 3).

3.3. Morphological analyses of Ti-Ag films

In order to reduce even more the strain in the metal conductor, without sacrificing the electrical performance and/or changing the amplitude or period of the design, the obtained results show that the number of zigzags can be further optimized (increased), increasing their number with several periods of smaller thickness or even with periods of varying thicknesses. This “multi trace” films may improve the stretchability and reduce the induced stresses [34]. Figure 5 shows the cross-section images of the sputtered GLAD samples, where all the films seem to exhibit a typical columnar microstructure. The tilting of columns increases with the incident angle α . Nonetheless, the incident angle α and the column angle β are not equal due to shadowing effects [31, 32]. As the total film thickness was kept approximately constant, with increasing number of zigzag periods, the single period thickness decreases. For an incident angle $\alpha = 40^\circ$, the obtained inclined (1/2 period zigzag) and zigzag architectures (1 and 2 periods) exhibit a weakly distinguishable columnar structure. The column angle β cannot be accurately determined for any zigzag period. It is in agreement with the quite dense structure typically observed in GLAD thin films prepared with incident angles lower than 60° . The shadowing effect is not relevant enough for incident angles lower than 60° . The oriented growth is favoured but insufficiently to produce a clear defined cross section morphology [31-33]. For incident angles α higher than 60° , inclined as well as zigzag columns are better viewed. The column angle is $\beta = 40^\circ$ and 45° (for any zigzag period) for a corresponding incident angle $\alpha = 60^\circ$ and 80° , respectively. These close β values are expected within the GLAD sputtering process due to the dispersion of sputtered particles (the latter do not have a ballistic trajectory because of the sputtering pressure required to maintain the plasma). As a result, the β angle tends to saturate in spite of an increase of the incident angle and the films do not exhibit significant changes of their cross section morphology. In addition, with increasing the incident angle from 0° to a maximum of 80° , the structures become less dense and compact and an enhancement of the inter-columnar spacing is

perceivable, independently of the number of periods. Moreover a closer look also reveals well defined columnar features for incident angles of 60° and 80° , particularly evident for $\alpha = 80^\circ$.

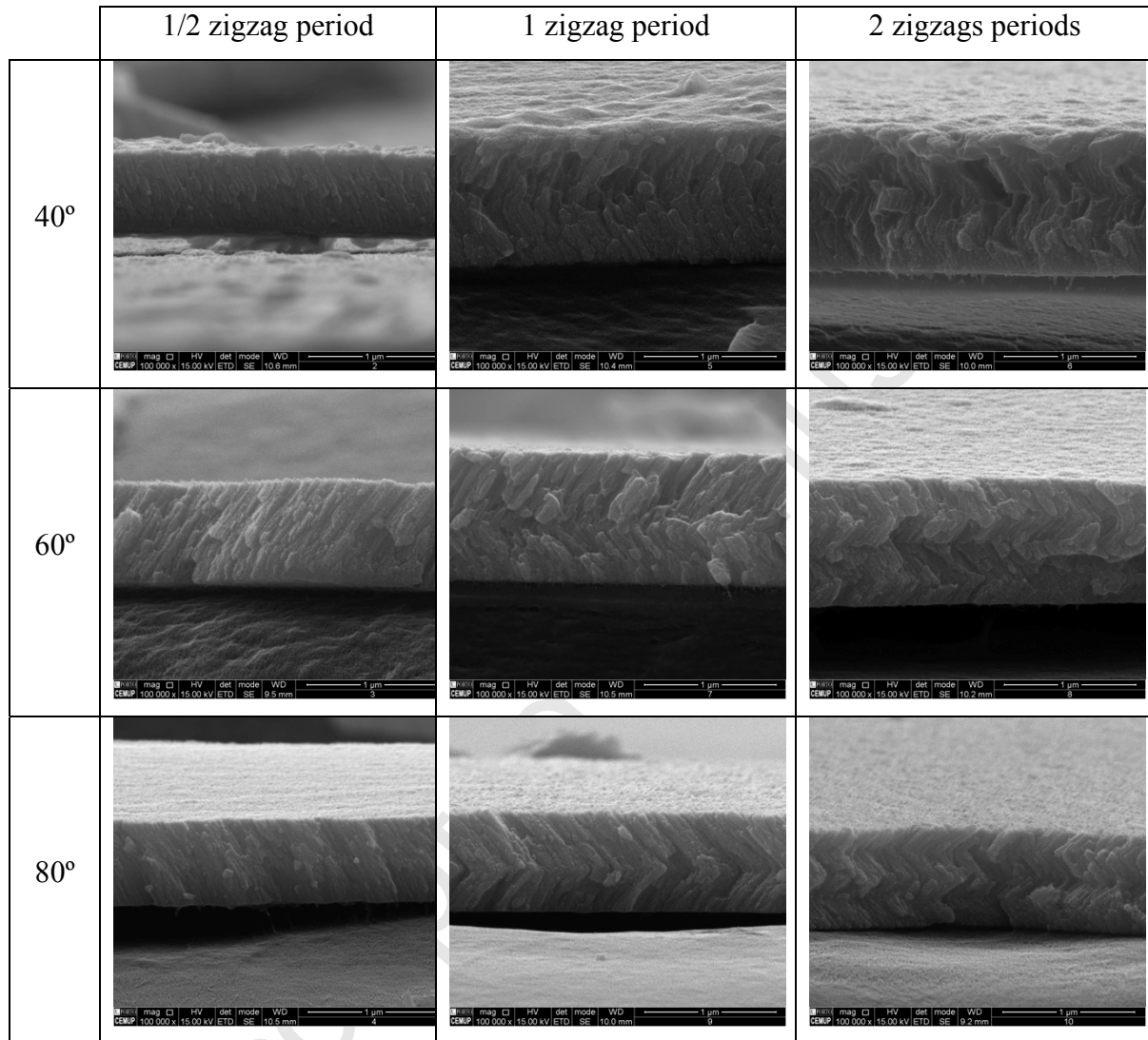


Figure 5 - SEM cross-section micrographs of the sputtered Ti-Ag samples for incident angles $\alpha = 0, 40, 60$ and 80° and $\frac{1}{2}, 1$ and 2 zigzags periods.

These results show the variations in the grain boundaries, mainly in the column frontiers which decreases the probability of the electron conduction [31] and consequently decreases the electrical conductivity.

AFM was used to characterize the morphology and surface roughness of the Ti-Ag samples with a scan area $5 \times 5 \mu\text{m}$. The influence of this α angle on the surface roughness is represented in Table 1.

Table 1: Surface roughness of the Ti-Ag films prepared with different incident angles of deposition and 2 zigzag periods.

Sample	Mean square roughness (R_q)	Mean roughness (R_a)	Max height (R_{max})
	<i>Nm</i>	<i>nm</i>	<i>nm</i>
$\alpha = 40^\circ$	8.4	6.7	61.7
$\alpha = 60^\circ$	5.8	3.5	73.1
$\alpha = 80^\circ$	6.8	5.1	86.6

Figure 6 and table 1 show that the surface of the samples prepared with an angle of deposition $\alpha = 60^\circ$ are the smoother ones with a rms roughness of 5.8 nm. The statistical mean roughness of the surface is about 3.5 nm, while the maximum height is about 73.1 nm. The results show maximum roughness for the samples prepared with $\alpha = 40^\circ$ and $\alpha = 80^\circ$ and therefore there is no relation between surface roughness and electromechanical response (Fig. 4b) but the latter is fully determined by the column angle.

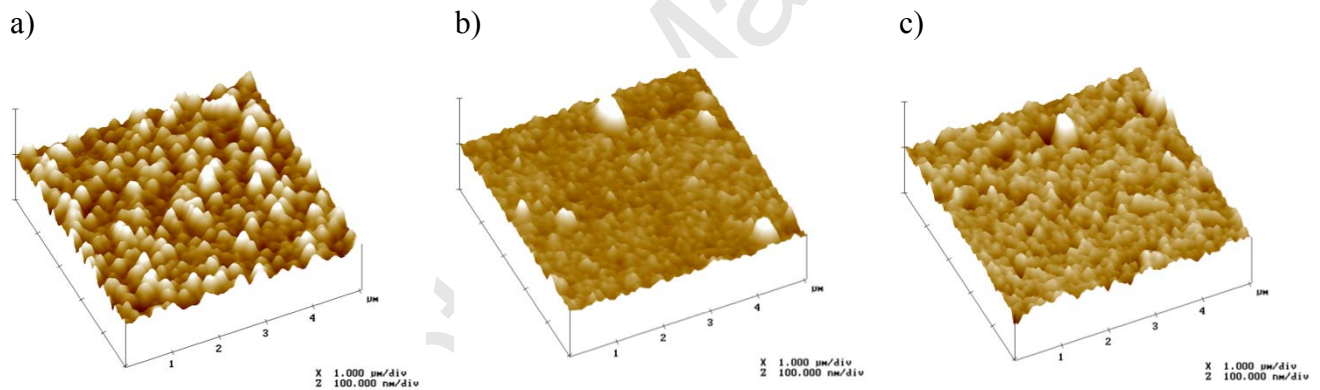


Figure 6 - AFM topographic images of sputtered Ti-Ag samples with 2 zigzag periods and for different incident angles: a) $\alpha = 40^\circ$; b) $\alpha = 60^\circ$; c) $\alpha = 80^\circ$.

3.4. Electromechanical response of the films

The electrical and piezoresistive response of carbon nanotube/poly(vinylidene fluoride) composites has been reported in [22]. The observed electrical and electromechanical responses are in accordance with the framework of the percolation theory. The piezoresistive response, quantitatively analysed by the gauge factor, is maximized at concentrations around the percolation threshold. In this region, the deformation of the composites induces strong and reversible variations in the CNT network and therefore in the electrical response. The maximum value of the gauge factor is 6.2 and the linearity of the response over a wide strain range shows the viability of these materials to be used as piezoresistive sensors. In the same

way, the piezoresistive response is stable with the number of cycles and reversible up to temperatures below 100 °C [22].

In this study, electromechanical tests on the Ti-Ag coated carbon nanotube/poly(vinylidene fluoride) composites were performed on composites with the same percentage of CNT (3 wt.%), i.e. around the percolation threshold, where the GF is the largest [22]. In this way, it was analysed whether the structure of the electrodes influences the signal response of the transducers. For this purpose, two parallel rectangular Ti-Ag electrodes of 6 mm width and 1 mm distance between them were coated onto one of the samples sides.

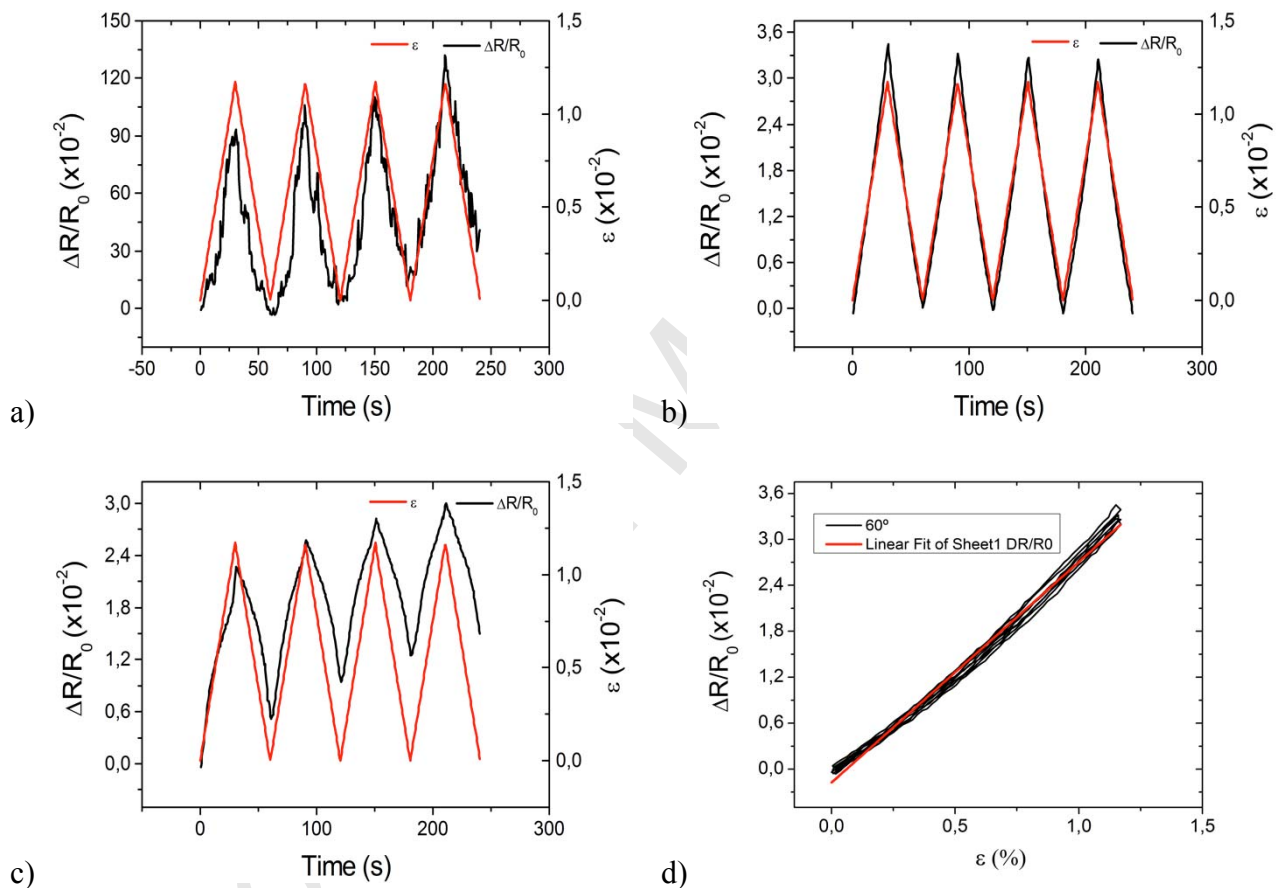


Figure 7 – Electromechanical response of samples prepared with 2 zigzag period Ti-Ag films deposited on PVDF substrates with 3 wt.% CNT. The z-deformation is 1 mm and the deformation velocity is 0.5 mm/min at room temperature. The incident angle is a) $\alpha = 40^\circ$; b) $\alpha = 60^\circ$, c) $\alpha = 80^\circ$ and d) representative resistance variation vs. strain curves and the corresponding fit for the determination of the Gauge Factor for the sample with $\alpha = 60^\circ$.

The stability of the piezoresistive response was analysed for the different GLAD Ti-Ag electrodes prepared with varying incident angles and number of zigzags. Fig. 7a, 7b and 7c) shows the strain tests performed in the samples with electrodes with 2 zigzag periods

prepared with an incident angle $\alpha = 40^\circ$, 60° and 80° . The 2 zigzag period samples were selected as they provide the most stable piezoresistive signal.

From Fig. 7d) one can observe that loading and unloading curves do not coincide during two successive cycles, given evidence of a mechanical hysteresis in these composites. The mechanical hysteresis in the composite decreases with increasing number of cycles, in particular for the first few cycles.

The increasing of the incident and column angles (α and β , respectively), from $\alpha = 0^\circ$ to $\alpha = 60^\circ$, as well as the number of zigzag periods enhances the electromechanical response. Above an incident angle of 60° there is a divergence between the loading and unloading cycles, due to strong changes in the mechanical behaviour of the Ti-Ag films, leading to a very poor resistance to stretching as shown in Fig. 3. These results show that the electrode structure has a pronounced influence on the electrical conductivity response of the polymer composite (e.g. variations on the resistivity) and therefore in the performance of the sensor.

As shown in Fig. 7d) the electrical resistance changes fairly linearly with the applied strain and that the linearity is maintained for the different cycles and for the different samples. The curves were thus fitted by linear regression. The GF is defined as the ratio of fractional change in electrical resistance to the fractional change in length (strain) [37]:

$$GF = \frac{\Delta R / R}{\Delta l / l} \quad (2)$$

In equation 2, R is the steady-state material electrical resistance before deformation and ΔR is the resistance change caused by the variation in length Δl [37]. The quantity l represents the length of the sample. The resistance change under strain results from the contribution of the dimensional change – geometrical effect ΔR_D - and from the intrinsic piezoresistive effect ΔR_I . For the surface mode measurements (Fig. 2b) the GF can be written as [37]:

$$GF = \frac{\Delta R / R}{\varepsilon} = \Delta R_D + \Delta R_I = (1 + \nu) + \frac{d\rho / \rho}{\varepsilon} \quad (3)$$

where, $\varepsilon = \Delta l / l$, ν is the Poisson ratio and ρ is the electrical resistivity.

The slope of the linear fit with equation is presented in table 2.

Table 2: GF values resulting of the linear fit of $\Delta R/R$ as function of stress ε for samples with 2 zigzags and PVDF substrates with 3 wt.% CNT.

Angle	GF	Standard Error
$\alpha = 40^\circ$	85	2
$\alpha = 60^\circ$	2.88	0.01
$\alpha = 80^\circ$	1.44	0.05

From Solef®PVDF datasheet, the Poisson ratio of PVDF is 0.35 at room temperature, which means that the geometric effect contribution to GF is around 1.35. Therefore, the obtained values of the GF , that are above this value (Table 2), show a strong intrinsic contribution of the CNT/polymer composite to the GF for the films prepared with $\alpha = 60^\circ$ and roughly negligible for $\alpha = 80^\circ$, as observed by comparison with the value of $GF \sim 1.35$ calculated from just geometrical factors. Further, the $\alpha = 40^\circ$ films show a strong intrinsic contribution from the electrodes themselves, as can be observed by maximum values of the GF obtained for these polymer composites with non-piezoresistive gold film, Table 3, data from [22].

Table 3: GF values resulting of the linear fit of $\Delta R/R$ as function of stress ε for samples with non-piezoresistive gold and PVDF substrates with CNT [22].

CNT (wt.%)	GF	Standard Error
1	2.63	0.19
1.3	3.75	0.09
1.7	6.18	0.30
2	4.84	0.07
3	1.54	0.18
7	1.13	0.01
10	1.70	0.18

For the samples prepared with gold films and concentrations above 3 wt.% CNT, the geometric factor is the dominant one, but just below 2 wt.% CNT loading, the intrinsic contribution to the GF is dominant. In the case of the Ti-Ag films, the change in conductivity induces strong variation of the response of the sensors due to their varying electrical response, which superimposes the variation of the piezoresistive composite [21, 38]. It can be further stated that whereas the electromechanical signal is mainly due to the polymer sensing

element for electrodes prepared with $\alpha = 60^\circ$ and 80° , the strong variations in resistivity under mechanical solicitation for the sample prepared with $\alpha = 40^\circ$ is ascribed to variation in the electrode itself. Upon stable response over varying cycles, the results shows a promising way to use the films as piezoresistive sensors themselves because the piezoresistive effects of the polymer material with non-piezoresistive gold had been studied [22], and the response of the piezoresistive films can be extrapolated by comparison. This is correlated with changes in the grain boundaries, mainly in the column frontiers which promote the tunneling resistance change [31]. The variation of the conductivity with angle α is mainly due to significant modifications of the film's morphology. The obtained values are reasonable for these types of composites; however, denser and compact structures with smoother surfaces showed a good strain distribution coupled with appropriate electrical conductivity, favoring the electromechanical response of the coated polymer. The best results were obtained when the polymer was coated with Ti-Ag films produced with intermediate incident angles.

4. Conclusions

Ti-Ag thin films were prepared with a systematic variation of the incident angle $\alpha = 40^\circ$, 60° and 80° and number of zigzag periods in order to be applied as electrodes in high strain piezoresistive polymer based composites based on CNT and PVDF. Upon uniaxial stretching, for the zigzag structures, the resistance starts increasing for strains up to 3 %, rising sharply for strains above 10 %, due to thin film mechanical and electrical failure. By increasing the number of zigzags, the change in conductivity of the Ti-Ag films induces strong variation of the response of the sensors due to their varying electrical response, which superimposes the variation of the response of the piezoresistive composite and the best results were obtained when the polymer was coated with intermediate incident angles ($\alpha = 60^\circ$). The results show that the electrodes structure has a pronounced influence on the overall sensor response leading to values of the GF up to 85 mainly due to the electromechanical contribution of the thin film, which stability has to be studied for potential use for sensor applications itself.

5. Acknowledgements

This work was supported by FEDER through the COMPETE Program and by the Portuguese Foundation for Science and Technology (FCT) in the framework of the Strategic Project PEST-C/FIS/UI607/2014 and the project Matepro –Optimizing Materials and Processes”, ref. NORTE-07-0124-FEDER-000037”, co-funded by the “Programa Operacional Regional do

Norte” (ON.2 – O Novo Norte), under the “Quadro de Referência Estratégico Nacional” (QREN), through the “Fundo Europeu de Desenvolvimento Regional” (FEDER). The authors also thank FCT for financial support under project PTDC/CTM-NAN/112574/2009. AF thanks the FCT for grant SFRH/BD/69796/2010.

6. References

- [1] G.T. Pham, Y.-B. Park, Z. Liang, C. Zhang, B. Wang, Processing and modeling of conductive thermoplastic/carbon nanotube films for strain sensing, *Polymer*, 39(2008) 209-16.
- [2] C. Li, E. Thostenson, T. Chou, Sensors and actuators based on carbon nanotubes and their composites: A review, *Composites Science and Technology*, 68(2008) 1227-49.
- [3] A. Ferreira, M.T. Martínez, A. Ansón-Casaos, L.E. Gómez-Pineda, F. Vaz, S. Lanceros-Mendez, Relationship between electromechanical response and percolation threshold in carbon nanotube/poly(vinylidene fluoride) composites, *Carbon*, 61(2013) 568-76.
- [4] S.D. Deshpande, K. Jaehwan, Y. Sung-Ryul, Studies on conducting polymer electroactive paper actuators: effect of humidity and electrode thickness, *Smart Materials and Structures*, 14(2005) 876.
- [5] S.M. Richardson-Burns, J.L. Hendricks, B. Foster, L.K. Povlich, D.-H. Kim, D.C. Martin, Polymerization of the conducting polymer poly(3,4-ethylenedioxythiophene) (PEDOT) around living neural cells, *Biomaterials*, 28(2007) 1539-52.
- [6] S. Wagner, S.P. Lacour, J. Jones, P.-h.I. Hsu, J.C. Sturm, T. Li, et al., Electronic skin: architecture and components, *Physica E: Low-dimensional Systems and Nanostructures*, 25(2004) 326-34.
- [7] S.P. Lacour, S. Wagner, R.J. Narayan, T. Li, Z. Suo, Stiff subcircuit islands of diamondlike carbon for stretchable electronics, *Journal of Applied Physics*, 100(2006) 014913.
- [8] D.S. Gray, J. Tien, C.S. Chen, High-Conductivity Elastomeric Electronics, *Advanced Materials*, 16(2004) 393-7.
- [9] R. Pelrine, R. Kornbluh, J. Joseph, R. Heydt, Q. Pei, S. Chiba, High-field deformation of elastomeric dielectrics for actuators, *Materials Science and Engineering: C*, 11(2000) 89-100.
- [10] M. Gonzalez, F. Axisa, M. Vanden, D. Brosteaux, B. Vandeveldel, J. Vanfleteren, Design of metal interconnects for stretchable electronic circuits, *Medical Biology (Helsinki)*, 48(2008) 825-32.
- [11] S. Rosset, H. Shea, Flexible and stretchable electrodes for dielectric elastomer actuators, *Appl Phys A*, 110(2013) 281-307.
- [12] C. Lopes, C. Gonçalves, P. Pedrosa, F. Macedo, E. Alves, N.P. Barradas, et al., TiAgx thin films for lower limb prosthesis pressure sensors: Effect of composition and structural changes on the electrical and thermal response of the films, *Appl Surf Sci*, 285, Part A(2013) 10-8.
- [13] C. Gonçalves, C. Lopes, C. Fonseca, A. Guedes, F. Vaz, Structural and morphological evolution in TiAgx thin films as a function of in-vacuum thermal annealing *Journal of Nano Research*, 25(2013) 67-76.
- [14] A. Ewald, S.K. Gluckermann, R. Thull, U. Gbureck, Antimicrobial titanium/silver PVD coatings on titanium, *Biomedical engineering online*, 5(2006) 1-10.

- [15] M. Takahashi, M. Kikuchi, Y. Takada, O. Okuno, Grindability and mechanical properties of experimental Ti–Au, Ti–Ag and Ti–Cu alloys, *International Congress Series*, 1284(2005) 326-7.
- [16] M. Kikuchi, M. Takahashi, O. Okuno, Machinability of Experimental Ti-Ag Alloys, *Dental Materials Journal*, 27(2)(2008) 216-20.
- [17] J.A. Thornton, The microstructure of sputter-deposited coatings, *Journal of Vacuum Science & Technology A: Vacuum, Surfaces, and Films*, 4(1986) 3059.
- [18] R. Messier, Revised structure zone model for thin film physical structure, *Journal of Vacuum Science & Technology A: Vacuum, Surfaces, and Films*, 2(1984) 500.
- [19] I. Petrov, P.B. Barna, L. Hultman, J.E. Greene, Microstructural evolution during film growth, *Journal of Vacuum Science & Technology A: Vacuum, Surfaces, and Films*, 21(2003) S117.
- [20] S. Mahieu, P. Ghekiere, D. Depla, R. De Gryse, Biaxial alignment in sputter deposited thin films, *Thin Solid Films*, 515(2006) 1229-49.
- [21] T.G. Knorr, R.W. Hoffman, Dependence of Geometric Magnetic Anisotropy in Thin Iron films., *Physical Review*, 113(1959) 1039-46.
- [22] A. Ferreira, J.G. Rocha, A. Ansón-Casaos, M.T. Martínez, F. Vaz, S. Lanceros-Mendez, Electromechanical performance of poly(vinylidene fluoride)/carbon nanotube composites for strain sensor applications, *Sensors and Actuators A: Physical*, 178(2012) 10-6.
- [23] A. Bottino, G. Capannelli, S. Munari, A. Turturro, Solubility parameters of poly(vinylidene fluoride), *Journal of Polymer Science Part B: Polymer Physics*, 26(1988) 785-94.
- [24] J. Mano, V. Sencadas, a. Costa, S. Lancerosmendez, Dynamic mechanical analysis and creep behaviour of β -PVDF films, *Materials Science and Engineering A*, 370(2004) 336-40.
- [25] N.P. Barradas, C. Jeynes, R.P. Webb, Simulated annealing analysis of Rutherford backscattering data, *Applied Physics Letters*, 71(1997) 291-3.
- [26] N.P. Barradas, C. Jeynes, M.A. Harry, RBS/simulated annealing analysis of iron-cobalt silicides, *Nuclear Instruments and Methods in Physics Research Section B: Beam Interactions with Materials and Atoms*, 136–138(1998) 1163-7.
- [27] P. Costa, J. Silva, V. Sencadas, R. Simoes, J.C. Viana, S. Lanceros-Méndez, Mechanical, electrical and electro-mechanical properties of thermoplastic elastomer styrene-butadiene-styrene/multiwall carbon nanotubes composites, *J Mater Sci*, 48(2013) 1172-9.
- [28] L.J.v.d. Pauw, A method of measuring specific resistivity and hall effect of discs of arbitrary shape., 13(1958) 1-9.
- [29] L.J.v.d. Pauw, A method of measuring the resistivity and hall coefficient on lamellae of arbitrary shape., *Philips Technical Review*, 20(1958) 220-4.
- [30] M.E. Day, M. Delfino, J.A. Fair, W. Tsai, Correlation of electrical resistivity and grain size in sputtered titanium films, *Thin Solid Films*, 254(1995) 285-90.
- [31] J. Lintymer, J. Gavaille, N. Martin, J. Takadoum, Glancing angle deposition to modify microstructure and properties of sputter deposited chromium thin films, *Surface and Coatings Technology*, 174-175(2003) 316-23.
- [32] J. Lintymer, N. Martin, J.-M. Chappe, J. Takadoum, Glancing angle deposition to control microstructure and roughness of chromium thin films, *Wear*, 264(2008) 444-9.
- [33] P. Pedrosa, C. Lopes, N. Martin, C. Fonseca, F. Vaz, Electrical characterization of Ag:TiN thin films produced by glancing angle deposition, *Materials Letters*, 115(2014) 136-9.

- [34] J.-Y. Rauch, F. Sthal, L.U.C. Carpentier, N. Martin, A. Besnard, Metal-to-dielectric transition induced by annealing of oriented titanium thin films, *Functional Materials Letters*, 06(2013) 1250051.
- [35] A.F. Mayadas, M. Shatzkes, Electrical-Resistivity Model for Polycrystalline Films: the Case of Arbitrary Reflection at External Surfaces, *Physical Review B*, 1(1970) 1382-9.
- [36] O.v.d. Sluis, Y.Y. Hsu, P.H.M. Timmermans, M. Gonzalez, J.P.M. Hoefnagels, Stretching-induced interconnect delamination in stretchable electronic circuits, *Journal of Physics D: Applied Physics*, 44(2011) 034008.
- [37] S. Beeby, G. Ensell, M. Kraft, N. White, *MEMS mechanical sensors*, Boston: Artech House; 2004.
- [38] A. Shokuhfar, P. Heydari, M.R. Aliahmadi, M. Mohtashamifar, S. Ebrahimi-Nejad R, M. Zahedinejad, Low-cost polymeric microcantilever sensor with titanium as piezoresistive material, *Microelectronic Engineering*, 98(2012) 338-42.

7. Biographies

Armando Ferreira received the B.Sc. and the M.Sc. degree in physics from the University of Minho, Braga, Portugal, in 2007 and 2010, respectively. He is currently working towards the Ph.D. at the Physics Department, University of Minho. His thesis work consists in the development of a pressure sensor network system for static and dynamic measurement. Application to the lower limb/prosthesis pressure mapping.

Cláudia Lopes graduated in Physics and Chemistry in 2003, obtained her Master degree in Physics in 2009, both conferred by Minho University, Portugal. Currently she is a Ph.D. student at the Physics Department, University of Minho. Her research work consists in the development and characterization of multifunctional coatings for biosensors devices.

Nicolas Martin obtained a Ph.D. in Physical Chemistry from the University of Franche-Comté in 1997 and an habilitation degree from the same University in 2005. He was a researcher at the Ecole Polytechnique Fédérale de Lausanne from 1998 to 2000 in the Physics department. He was nominated as Assistant Professor at the National Engineering School ENSMM – “Ecole Nationale Supérieure de Mécanique et des Microtechniques in Besançon in 2000, and Full Professor in 2008. His research is focused on the physics and technology of metallic and ceramic thin films prepared by reactive sputtering. He is also interested in nanostructuring of coatings prepared by Glancing Angle Deposition (GLAD). He was the head of the Micro NANO MAterials & Surfaces team (MINAMAS) in the Micro Nano

Sciences & Systems (MN2S) research department of the FEMTO-ST Institute for 2008 and 2009. He is now one of the Deputy Directors of MN2S research department.

S. Lanceros-Mendez graduated in physics at the University of the Basque Country, Leioa, Spain, in 1991. He obtained his Ph.D. degree in 1996 at the Institute of Physics of the Julius-Maximilians-Universität Würzburg, Germany. He was Research Scholar at Montana State University, Bozeman, MT, from 1996 to 1998 and visiting scientist at the A.F. Ioffe Physico-Technical Institute, St. Petersburg, Russia (1995), Pennsylvania State University, USA (2007) and University of Potsdam (2008). Since September 1998 he has been at the Physics Department of the University of Minho, Portugal, where he is an Associate Professor. His work is focused in the area of electroactive smart materials and its applications as sensors and actuators with more than 150 research papers and several patents.

José Filipe Vilela Vaz graduated in Physics and Chemistry at the University of Minho, UM, Braga, Portugal in 1992, where he obtained also his Ph.D. degree in Physics in 2000. Since September 1992 he has been working at the Physics Department of UM, involved in research areas related with thin films and their application. Main research topics concern hard nanostructured thin films, with targeted applications varying from tools and machine parts, including polymers. From 2001 he is also developing new optical thin film systems, based on oxynitrides, oxycarbides, and their mixing. Materials with Surface Plasmon Resonance behavior are also investigated.

Figure captions

Figure 1 - Schematic representation of the thin film microstructural features.

Figure 2 - Schematic representation of the experimental configuration of the a) clamps for the stress-strain uniaxial stress experiments (method 1) with simultaneous electrical measurements for electrical response evaluation of the samples and b) representation of the 4-point bending tests (method 2) apparatus where z is the vertical displacement, d is the thickness of the sample and a is the distance between the first and the second bending points (15 mm). The electrodes are in the center of the sample.

Figure 3 - Electrical conductivity of Ti-Ag films as a function of the incident angle (α) and the number of periods, and electrical conductivity of polymer composite as a function of CNT (wt.%).

Figure 4 - Electrical resistance as a function of the tensile strain ϵ of the sputtered Ti-Ag samples for the different incident angles $\alpha = 0, 40, 60$ and 80° and geometries: a) 1 zigzag period; b) 2 zigzags periods.

Figure 5 - SEM cross-section micrographs of the sputtered Ti-Ag samples for incident angles $\alpha = 0, 40, 60$ and 80° and $\frac{1}{2}, 1$ and 2 zigzags periods.

Figure 6 - AFM topographic images of sputtered Ti-Ag samples with 2 zigzag periods and for different incident angles: a) $\alpha = 40^\circ$; b) $\alpha = 60^\circ$; c) $\alpha = 80^\circ$.

Figure 7 – Electromechanical response of samples prepared with 2 zigzag period Ti-Ag films deposited on PVDF substrates with 3 wt.% CNT. The z-deformation is 1 mm and the deformation velocity is 0.5 mm/min at room temperature. The incident angle is a) $\alpha = 40^\circ$; b) $\alpha = 60^\circ$, c) $\alpha = 80^\circ$ and d) representative resistance variation vs. strain curves and the corresponding fit for the determination of the Gauge Factor for the sample with $\alpha=60^\circ$.

Highlights

- Thin films prepared with specific architectures (columns and zigzag profiles), carried out by Glancing Angle Deposition, GLAD
- The influence of thin film architectures were correlated with respect to the performance of piezoresistive sensors, based on carbon nanotube/poly(vinylidene fluoride), CNT/PVDF, composites
- Electromechanical tests showed a behaviour that not corresponds to required response in pressure sensors but also a very different result when compared to conventional-like deposited thin films
- Thin film architectures have pronounced influence in the overall sensor response.